Received: 25 August 2020 | Revised: 2 February 2021 | Accepted: 10 February 2021

DOI: 10.1002/jbm.a.37156

ORIGINAL ARTICLE

Fabrication of hybrid scaffolds obtained from combinations of PCL with gelatin or collagen via electrospinning for skeletal muscle tissue engineering

Victor Perez-Puyana[1,2] | Paul Wieringa[2] | Yaiza Yuste[3] | Fernando de la Portilla[3] | Antonio Guererro[1] | Alberto Romero[1] | Lorenzo Moroni[2]

[1]Departamento de Ingeniería Química, Universidad de Sevilla, Facultad de Química, Escuela Politécnica Superior, Sevilla, Spain

[2]Department of Complex Tissue Regeneration, MERLN Institute for Technology-Inspired Regenerative Medicine, Maastricht University, Maastricht, The Netherlands

[3]Departamento de Cirugía, Institute of Biomedicine of Seville (IBiS), "Virgen del Rocío" University Hospital, IBIS CSIC/ University of Seville, Sevilla, Spain

Correspondence
Lorenzo Moroni, Department of Complex Tissue Regeneration, MERLN Institute for Technology-Inspired Regenerative Medicine, Maastricht University, 6200 MD, Maastricht, The Netherlands.
Email: l.moroni@maastrichtuniversity.nl

Funding information
Ministerio de Economia y Competitividad, Grant/Award Number: CTQ2015-71164-P

Abstract

The creation of skeletal muscle tissue in vitro is a major topic of interest today in the field of biomedical research, due to the lack of treatments for muscle loss due to traumatic accidents or disease. For this reason, the intrinsic properties of nanofibrillar structures to promote cell adhesion, proliferation, and cell alignment presents an attractive tool for regenerative medicine to recreate organized tissues such as muscle. Electrospinning is one of the processing techniques often used for the fabrication of these nanofibrous structures and the combination of synthetic and natural polymers is often required to achieve optimal mechanical and physiochemical properties. Here, polycaprolactone (PCL) is selected as a synthetic polymer used for the fabrication of scaffolds, and the effect of protein addition on the final scaffolds' properties is studied. Collagen and gelatin were the proteins selected and two different concentrations were analyzed (2 and 4 wt/vol%). Different PCL/protein systems were prepared, and a structural, mechanical and functional characterization was performed. The influence of fiber alignment on the properties of the final scaffolds was assessed through morphological, mechanical and biological evaluations. A bioreactor was used to promote cell proliferation and differentiation within the scaffolds. The results revealed that protein addition produced a decrease in the fiber size of the membranes, an increase in their hydrophilicity, and a softening of their mechanical properties. The biological study showed the ability of the selected systems to harbor cells, allow their growth and, potentially, develop musculoskeletal tissues.

KEYWORDS
collagen, electrospinning, PCL, scaffolds, skeletal muscle cells

1 | INTRODUCTION

Total muscle tissue represents 40% of the human body and is part of those structures in our body that are highly adapted to their function, limiting their ability to restore themselves after damage.[1] Skeletal muscle cells are cylindrical and very elongated; their size varies from 10 to 100 μm and their length varies from 1 to 50 mm. The plasma membrane (also called sarcolemma) is surrounded by a basement membrane consisting of a basal lamina and a layer of reticular fibers. Each muscle cell contains numerous nuclei elongated in the fiber

direction and arranged on its periphery. There are other nuclei also located in the cellular periphery, below the basal lamina, which are not part of the muscle cells, but of the adjoining cells called satellite cells.[2] The creation of skeletal muscle tissue in vitro is one of the topics of greatest interest in recent times in the field of biomedical research; however, despite the advancements that have been made, determining the biophysical conditions that must be applied to the cellular environment to achieve muscle regeneration is still a challenge today.[3-6]

Toward this aim, the use of biomaterial support structures, or scaffolds, to facilitate to formation of muscle in vitro is an active area of research. The field of biomaterials has grown exponentially and the field has evolved from earlier studies in the 1970s and 1980s focused on the development of bioinert materials to more recent studies from the last decade devoted to more sophisticated biomaterials designed to interact with cells, giving rise to structures that resemble the tissues to be replaced.[7] Thus, tissue engineering emerged as the science of designing and manufacturing new tissues for the functional restoration of altered native ones and the replacement of damaged structures. The biomaterials used in tissue engineering can be processed by different techniques to generate a variety of different scaffold structures, such as self-assembly, freeze-drying, 3D printing, or electrospinning.[8-11]

Electrospun structures present a very high surface area, making these structures a suitable candidate for cell adhesion, proliferation and differentiation, which is essential to guide tissue formation.[12,13] Polymeric electrospun scaffolds have been used for different specific applications in tissue engineering. As examples, PVA scaffolds were studied for neural tissue engineering,[14,15] polystyrene was used to study osteosarcoma cell adhesion[16] or polyethylene oxide for drug delivery purposes.[17] Specifically, the nature of musculoskeletal diseases is complex and encompasses a wide spectrum of pathologies that affect different connective tissues of the skeletal system, including bones, cartilage, muscles, tendons, and ligaments. Due to the lack of knowledge of the etiopathology of many of these diseases, treatment options are limited in most cases to the control of their symptoms rather than their cure or prevention.[18] A possible solution could be the use of electrospun scaffolds because its use for muscle application may fulfill the needs for musculoskeletal diseases, highlighting the alignment which could promote cell organization.

In addition to specific requirements for scaffold development, there are still unresolved challenges in the development of multifunctional scaffolds that exhibit functionally contractile muscle cells, such as vascularization problems, nerve regeneration, electromechanical coupling, and structural, mechanical and electrophysiological properties. The main disadvantage, particularly in the production of musculoskeletal tissues, is the absence of physiological and mechanical stimuli during their formation, which prevents adequate cell regulation and spatial development of the tissue, with the consequent decrease in its mechanical quality.[19,20] These drawbacks could be solved by the use of a bioreactor to induce a mechanical stimuli to the scaffolds, allowing a better cell proliferation.[21] In general, most tissue engineering bioreactors share the same basic functions: maintaining asepsis, controlling temperature and pH, as well as applying physico–chemical stimuli to induce proliferation and differentiation.[22] In fact, as an example, Akhyari et al. (2002) proved that cyclic mechanical stimuli enhance the formation of bioengineered cardiac muscle grafts.[23]

Our hypothesis is that electrospun PCL-based scaffolds could be combined with gelatin or collagen in order to obtain more hydrophilic structures to promote cell adhesion, as well as scaffolds with tunable mechanical properties that are suitable for use in combination with an in vitro bioreactor for muscle tissue maturation. The approach adopted in this study is to compare the effect of two biopolymers (collagen and gelatin) in combination with PCL to tune the properties of PCL fibers, together with the analysis of the influence of fiber alignment to produce scaffolds with potential application in skeletal muscle tissue engineering.

Poly(ε-caprolactone) (PCL) is one of the most used biodegradable polymer in biomedical applications and it was approved by the FDA for uses in several biomedical applications ranging from drug delivery to implantable devices.[24] PCL with a high molecular weight (80,000 g/mol) has been widely considered due to its biocompatibility, suitable mechanical properties and easy processing.[25,26] Hendrikson et al. (2015) produced PCL scaffolds with different molecular weight for mesenchymal stromal cell differentiation.[27] Similar structures were processed by Gumusderelioglu et al. (2011) for dermal applications.[25] On the other hand, PCL has also been considered as raw material for other applications, such as materials with antimicrobial properties.[28] However, PCL has some drawbacks, such as its hydrophobicity and its low degradation rate, which limit its cell interaction and post-implant resorption, respectively. PCL has also a high stiffness that this semi-crystalline polymer imparts to the resulting fabricated scaffold structures. Therefore, it has been used in combination with other biopolymers to enhance the properties of the resultant scaffolds.[29-31]

Among the different proteins and polysaccharides that can be used as natural polymers, it is worth highlighting collagen, which is found in many biological structures. Among the different collagen types, Type I collagen is the most abundant, being present in bones, tendons, skin, and ligaments, among several others. It is formed by two identical α1-chains and one α2(I)-chain (heterotrimers).[32] On the other hand, gelatin, which is the denatured form of collagen, is obtained by acidic or alkaline processing and thermal denaturation of collagen. It is widely used as a scaffold material due to its advantageous biomechanical properties and biocompatibility in several tissue engineering applications.[32]

Binary PCL-based systems have been studied, such as the investigation conducted by Hartman et al. (2010) about the biofunctionalization of PCL-based scaffolds to produce a 3D-pharmacokinetic model or the formation of PCL/gelatin membranes by Ren et al. (2017) for bone regeneration.[29,33] Ternary structures were also produced, such as the studies of Aguirre-Chagala et al. (2017) and Chong et al. (2019), producing ternary scaffolds formed by PCL, collagen and elastin.[24,34] However, the main drawback of those scaffolds is the high stiffness of the resulting fibers, making them not suitable for tissue engineering application, in which mechanical stimuli is a key factor for cell growth.

In addition to the initial formulation, it is important to select the optimal working parameters, as they influence the properties of

the resulting fibers. The processing conditions involved in the electrospinning process are voltage, needle-collector distance, flow rate, collector modality (e.g., flat plate versus rotating mandrel), and even environmental parameters, such as temperature and humidity. In our chosen setup of a rotating mandrel collector, the rotational speed of the collector is a crucial processing variable that affects both the size and the orientation of the fibers. This results in aligned fiber membranes that allow modifying the mechanical and structural properties of these membranes.[35] The resulting scaffolds encourage the oriented growth of the cells in these structures, as shown by Meng et al. (2010) with combinations of PLGA and gelatin to study the proliferation of mouse osteoblasts.[36]

In this work, we used a bioreactor to stimulate low molecular weight PCL-based (45,000 g/mol) scaffolds, allowing cell growth and differentiation for skeletal muscle tissue engineering. Furthermore, a complete mechanical evaluation of the scaffolds, which encompasses the analysis of the mechanical properties and cyclic loading tests conducted under dry and wet conditions, was also performed.

Thus, this study proposes the development of polymeric membranes based on PCL and proteins (gelatin and collagen) by electrospinning with the aim of modeling and evaluating their influence on the mechanical, physicochemical and microstructural properties of the obtained fibers. In addition, the most suitable combination was selected for the assessment of the alignment for musculoskeletal tissue engineering. Uniaxial tensile strength tests and SEM imaging were performed. In addition, contact angle measurements and a biological analysis were also carried out.

2 | MATERIAL AND METHODS

2.1 | Materials

The gelatin protein used (Gel) was fish gelatin type B (80-120 g Bloom), supplied by Henan Boom Gelatin Co. Ltd (China). It presented a protein content of ~98 wt% and was also composed of lipids and moisture with a content of less than 1 wt%. On the other hand, collagen protein (Col) was supplied by Essentia Protein Solutions (Grasten, Denmark). It presented a protein content of ~ 95 wt% and other components, such as lipids and moisture (less than 1 wt%). Poly(ε-caprolactone) (M_w = 45,000 g/mol) and 1,1,1,3,3,3-hexafluoro-2-propanol (HFIP) were purchased from Sigma Aldrich (Germany).

2.2 | Electrospinning process

Different solutions with PCL and collagen or gelatin were prepared to study the influence of gelatin and collagen on PCL scaffolds. Solutions with different protein content (2 and 4 wt/vol%; named as 2 and 4%) and a constant concentration of PCL (16 wt/vol%; named as 16%), according to Sant et al. (2011),[30] were processed using HFIP as solvent. The solutions were prepared at room temperature by stirring for ~ 24 hr using a magnetic stirrer, before the electrospinning process. Once the different solutions were prepared, the electrospinning process was carried out in vertical mode using a Fluidnatek LE-100 equipment (Bioinicia).

Electrospinning allows the formation of nanofibrous membranes by the application of an electric field between the syringe, where the polymer solution is placed, and the collector. During this process, a jet of polymer solution is electrostatically extruded from the syringe needle to the collector, during which time the jet experiences a whipping instability that allows enough time for the solvent to evaporate, resulting in the formation of fibers.[37] The adequate processing conditions (voltage, flow rate, working distance, humidity, and temperature) were selected to produce suitable fibers. A nonwoven polyurethane mesh (6,691 LL, 40 g/m^2) was previously prepared by punching 12 mm circular holes and placed on the collector, filling the aluminum foil that covers the collector. Afterwards, the electrospinning process was performed at 14 kV using a 10 ml syringe with a 18G stainless steel needle (inner diameter 0.5 mm, Unimed S.A.), with a flow rate of 0.4 ml/hr and a needle-collector distance of 14 cm. The temperature and humidity were set at 25°C and 40%, respectively.

2.3 | Characterization of nanofibrous scaffolds

2.3.1 | Fourier transform infrared spectroscopy (FTIR)

The chemical bonds were analyzed by attenuated total reflectance (ATR)-FTIR using an iS50 ATR-FTIR spectrophotometer (Nicolet). The different spectra were collected in the range of 4,000–500 cm^{-1}. The measurements were carried out by placing the scaffolds in an ATR accessory providing an analysis of the surface.

2.3.2 | Water contact angle (WCA)

The scaffolds' wettability and hydrophobicity were assessed by WCA measurements using the sessile drop method (droplets with an approximate volume of 5 μl). Both WCA values of the right and left sides of the deionized water droplets were measured and the average value was calculated. The equipment used was a Drop Shape Analyzer (Krüss).

2.3.3 | Scanning electron microscopy (SEM)

Microscopy examination of scaffolds was assessed with a XL 30 (Philips XL Series) at an acceleration voltage of 15 kV. The samples were fixed onto an aluminum stub with a carbon sticker and sputter-coated with gold using the 108 auto (Cressington Scientific Instruments). A digital processing software, ImageJ, was used to determine the membrane porosity as well as the size of the fibers.

Apart from the SEM imaging, the atomic composition of the membranes was examined with the energy dispersive spectroscopy

capability of the XL 30 equipment using an EDAX Si(Li) detector at an acceleration voltage of 5 kV.

2.3.4 | Tensile strength measurements

Uniaxial tensile tests were performed using an ElectroForce 3200 (TA Instruments), evaluating the evolution of the tensile load with the strain. The measures were carried out using the ElectroForce low-force axial transducer 45N (10lbf) (TA Instruments). The extensional rate was 0.1 mm s^{-1} at 20°C. The samples were cut in a rectangular shape and placed in the ElectroForce clamps with sandpaper to avoid sample fracture. From the different measurements, three parameters were obtained: the maximum stress, the strain at break and Young's modulus.

2.4 | Biological evaluation of nanofibrous scaffolds

Three scaffolds were biologically evaluated to assess cell behavior. The cells used were rat skeletal myoblasts obtained from Rattus Norvegicus L6 cell line (ATCC® CRL-1458™) and were cultured in an incubator at 37°C in the presence of 5% CO_2 at the Instituto de Biomedicina de Sevilla (IBiS). The growth medium used was Minimum Essential Medium α (12571-063, Gibco) supplemented with 10% fetal bovine serum (F7524, Sigma) and 1% penicillin–streptomycin (15140–122, Gibco). After the cells reached 85–90% of confluence, they were sub-cultured using trypsin–EDTA at 0.05% (25300-062, Gibco) and 10×10^6 cells were seeded in each scaffold with growth medium, as it can be seen in Figure S4. The scaffolds were cultured in a TC3 bioreactor (EBERS Medical Technology SL, Spain) to be mechanically stimulated, inside the incubator, for 14 days. The culture medium was replaced every 48 hr. The scaffolds were processed and stained with haematoxylin–eosin (H&E) (GHS316 *Hematoxylin Solution*, Gill No. 3; HT110116 500ML: *Eosin Y Solution*) and immunohistochemically labeled with smooth muscle actin antibody (SMA) (*Actin, Smooth Muscle [1A4] Mouse Monoclonal Antibody*, Cell Marque) for histological analysis. The microscopy images were obtained using the Olympus IX-61 microscope.

From the different images, the evaluation of cell proliferation and cellular and tissue growth was carried out. In addition, cell viability was also calculated by estimating the percentage of living cells with respect to the areas of necrosis. Furthermore, the degree of cell differentiation was obtained by analyzing the immunohistochemical images.

2.5 | Statistical analysis

At least three replicates were carried out for each measurement. Statistical analyses were performed with *t* tests and one-way analysis of variance ($p < .05$) using the PASW Statistics for Windows (Version 18: SPSS, Chicago, IL). Standard deviations were calculated for selected parameters.

3 | RESULTS

3.1 | Influence of the addition of collagen and gelatin

3.1.1 | Physicochemical characterization of nanofibrous scaffolds

The presence of protein in the network of the fibrous membrane can be identified by the presence of nitrogen. Thus, an EDAX analysis of the obtained SEM images was performed to confirm whether the electrospun fibers contained proteins in their structure. The nitrogen present in the surface obtained from the EDAX profiles is shown in Table S1.

Furthermore, the presence of protein in the scaffolds was also measured via FTIR profiles (Figure S1). Figure S1A shows the profiles for the systems with PCL and PCL/gelatin (2 and 4%), whereas Figure S1B shows the profiles for the systems with PCL and PCL/collagen (2 and 4%).The spectrum of the PCL system shows two important areas: bands at 2,950 and 2,860 cm^{-1} related to the CH_2 symmetrical and asymmetrical stretching, and bands in the range of 1,450–1,000 cm^{-1} (C—H bending and wagging). The main area is the sharp band that appears at 1,725 cm^{-1}, associated with carbonyl stretching (characteristic of PCL).

However, the other systems (combination of PCL and gelatin or collagen) presented a different profile, with a broad area at ca. 3,280- cm^{-1} associated with N—H stretching (amide A signal), and bands at 1,635 and 1,525 cm^{-1} related to carbonyl stretching and C—N stretching of amides, respectively. However, the characteristic band for N—H bending (at $\sim$ 1240 cm^{-1}) is overlapped with the bands related to the CH_2 symmetrical and asymmetrical stretching in the 1,450–1,000 cm^{-1} range (C—H bending and wagging).[38] A summary of the main peaks obtained is shown in Table S2.

The wettability of the produced scaffolds was measured to study the effect of gelatin and collagen on the hydrophobicity of the scaffold. The evolution of the contact angle with the addition of gelatin or collagen is shown in Figure S2. PCL scaffolds were quite hydrophobic, presenting a contact angle of $\sim$ 105°. Comparing the different systems evaluated, those obtained with a gelatin concentration of 2 and 4% presented the best contact angle values (55 ± 2° and 52 ± 1°, respectively). In contrast, an interesting effect occurred when the protein used was collagen instead of gelatin: the addition of collagen did not produce a decrease in the contact angle of scaffolds. In fact, a slight increase of 3.5% (from 104.5° to 108.2°) was observed.

3.1.2 | Microstructural characterization of nanofibrous scaffolds

Figure S2 shows the SEM images of electrospun mats obtained as a function of the content of gelatin (Figures S2B and S2C for 2 and 4%, respectively) and collagen (Figures S2D and S2E for 2 and 4%, respectively). From the analyzed images, the porosity and the mean fiber size

were calculated (Table S1). Fiber size decreased with the addition of a protein, especially in the collagen-based scaffolds. For both collagen and gelatin-based scaffolds, the fiber diameters were significantly smaller as protein content increased up to 4%. While there were no significant differences when comparing fiber diameter of PCL/gelatin and PCL/collagen scaffolds with the same protein concentration.

The analysis of the fiber size distribution (Figure S2) revealed that all scaffolds had a Gaussian distribution with respect to a central value (ranging between 0.3 and 0.5 μm). Specifically, the use of collagen produced, in general, fibers with a lower mean fiber size and greater variability. On the other hand, the scaffolds produced with 4% of gelatin can be highlighted from the others as they showed a much more homogeneous distribution with most of the fibers in the range of 300–350 nm.

The pore area of the scaffolds was also evaluated (Table S1). All the systems presented pore area values between 700 and 1,100 nm^2. Although it is true that the addition of proteins to the system produced a decrease in the porosity of the scaffold, an increase in protein concentration produced no significant differences in the values obtained.

3.1.3 | Mechanical characterization of nanofibrous scaffolds

Figure S3 shows the profiles of the different systems processed (Figure S3A) and the different parameters measured from the mechanical testing (Figure S3B–D). All the systems showed a similar profile, with an initial region with a high constant stress–strain slope, which corresponds to the elastic region. This was followed by a long plastic region with a continuous decrease in the stress–strain slope toward a constant value. After reaching the maximum stress and strain at break, the samples broke with a sudden decrease in stress.

The analysis of the different parameters obtained from the strain–stress curves showed that the addition of a protein produced a decrease in both Young's modulus and maximum stress, compared to the values obtained for pure PCL scaffolds. This effect was more pronounced when the protein concentration was 4%. Interestingly, the same decrease of 56 and 85% for the gelatin and collagen systems, respectively, occurred in both Young's modulus and maximum stress. However, the effect on the strain at break differed depending

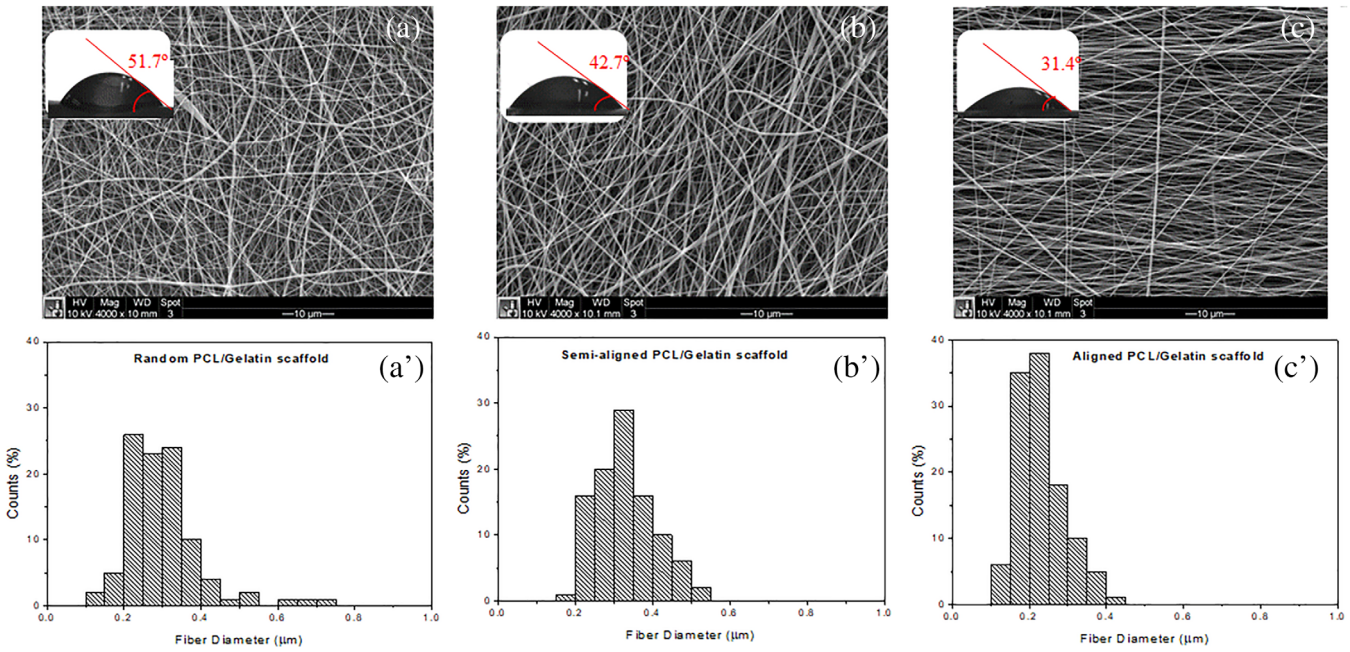

FIGURE 1 Contact Angle, scanning electron microscopy (SEM) images of the polycaprolactone (PCL)/gelatin scaffolds with different fiber alignments: (a) random, (b) semi-aligned and (c) aligned; fiber size distribution of the PCL/gelatin scaffolds with different alignments: (a') random, (b′) semi-aligned and (c′) aligned

TABLE 1 Alignment, mean fiber diameter, uniformity, pore area and contact angle values of the PCL/gelatin scaffolds obtained with different alignments: random, semi-aligned and aligned

SYSTEM	Alignment	Fiber size (nm)	Uniformity (%)	Pore area (nm^2)	Contact angle (°)
Random PCL/gelatin scaffold	0.13 ± 0.03 ^{A}	307 ± 89 ^{a}	71	780 ± 420 $^{\alpha}$	51.7 ± 1.5 ^{I}
Semi-aligned PCL/gelatin scaffold	0.40 ± 0.04 ^{B}	265 ± 35 ^{a}	87	1856 ± 994 $^{\alpha}$	42.7 ± 0.6 ^{I}
Aligned PCL/gelatin scaffold	0.75 ± 0.02 ^{C}	235 ± 68 ^{a}	71	913 ± 571 $^{\alpha}$	31.4 ± 1.6 ^{I}

Note: Values with different letters are significantly different ($p < .05$).
Abbreviation: PCL, polycaprolactone.

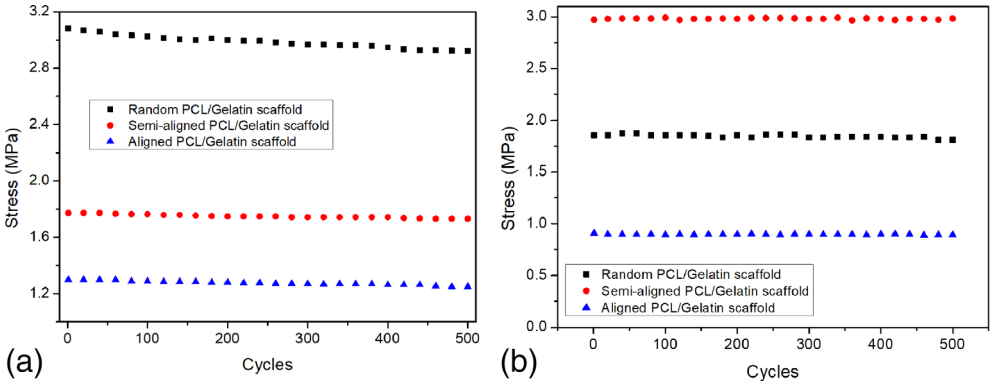

FIGURE 2 Profiles of the evolution of the stress of the polycaprolactone (PCL)/gelatin scaffolds produced with different alignments (random, semi-aligned and aligned) during a cyclic loading of 500 cycles at constant strain (10%) and frequency (1 Hz) in both dry and wet conditions

TABLE 2 Evolution of the stress of the PCL/gelatin scaffolds produced with different alignments (random, semi-aligned and aligned) during a cyclic loading of 500 cycles at a constant strain (10%) and frequency (1 Hz) in both dry and wet conditions

SYSTEM	Conditions	Initial stress (MPa)	Final stress (MPa)	% decrease
Random PCL/gelatin scaffold	Dry	3.08 ± 0.23	2.92 ± 0.39	5.2%
	Wet	2.98 ± 0.37	2.97 ± 0.28	0.4%
Semi-aligned PCL/gelatin scaffold	Dry	1.77 ± 0.05	1.73 ± 0.07	2.3%
	Wet	1.84 ± 0.15	1.81 ± 0.16	1.6%
Aligned PCL/gelatin scaffold	Dry	1.30 ± 0.15	1.25 ± 0.13	3.9%
	Wet	0.91 ± 0.24	0.89 ± 0.12	2.2%

Abbreviation: PCL, polycaprolactone.

on the protein used. The addition of gelatin produced a tendency to increase the strain at break, whereas the addition of collagen decreased it.

3.2 | Influence of the alignment of electrospun scaffolds

The PCL/gelatin (4%) system was selected to perform a study with varying rotational speed (0, 300 and 600 rpm), obtaining scaffolds with different alignment: Random (at 0 rpm), semi-aligned (at 300 rpm), and aligned (at 600 rpm).

The shape and structure of the scaffolds were analyzed by SEM (Figure 1(a), (b), and (c)). Furthermore, the alignment, mean fiber diameter, uniformity, porosity, and pore area were evaluated and summarized in Table 1. Homogeneous fibers with different alignment (0.13, 0.40, and 0.75) were obtained when the rotational speed was modified in the electrospinning process (the uniformity of the fiber size was over 70% for all the analyzed systems). Initially, the fibers were randomly oriented, but when the rotational speed was higher than 300 rpm (semi-aligned, Figure 1(b),(c)), a more organized latticework was obtained with more aligned fibers. In general, the increase in the rotational speed produced a slight decrease in the size of the fibers, although the differences between them were not significant ($p < .05$). In addition to the alignment and mean fiber size, fiber size distribution is also shown in Figure 1 (Figure 1(a),(b'), and (c') for the random, semi-aligned, and aligned systems, respectively). The results demonstrate that all systems presented a Gaussian distribution with respect to a central value (ranging between 200 and 400 nm).

In addition to obtaining thinner fibers, the increase in the alignment led to scaffolds formed by more homogeneous fibers, which can be seen by the narrowing of the Gaussian bell curve shown in the fiber size distribution graphs. Interestingly, the uniformity of the systems was above 70%, highlighting the semi-aligned scaffold with a uniformity higher than 85%.

On the other hand, the porosity of the scaffolds was also evaluated by means of the pore area (Table 1). All the systems presented pore area values between 800 and 1,900 nm^2, showing a significant increase for the semi-aligned system.

The wettability of the scaffolds produced with different alignments was evaluated via contact angle measurements (Figure 1). The results showed that the scaffolds produced with PCL and gelatin presented a highly hydrophilic character with contact angle value of approximately $\sim 50^{\circ}$.

In addition to standard mechanical characterization under dry conditions, the mechanical properties of the scaffolds were also measured in a wet condition (PBS buffer) to mimic the use of scaffolds in tissue engineering that are placed in a bioreactor and subject to mechanical stimuli. Following the same idea, the mechanical properties of the scaffolds were measured before and after a cyclic loading test to study the influence of the cyclic loading on them. Thus, uniaxial tensile tests were carried out before and after a cyclic loading test for each system (random, semi-aligned, and aligned).

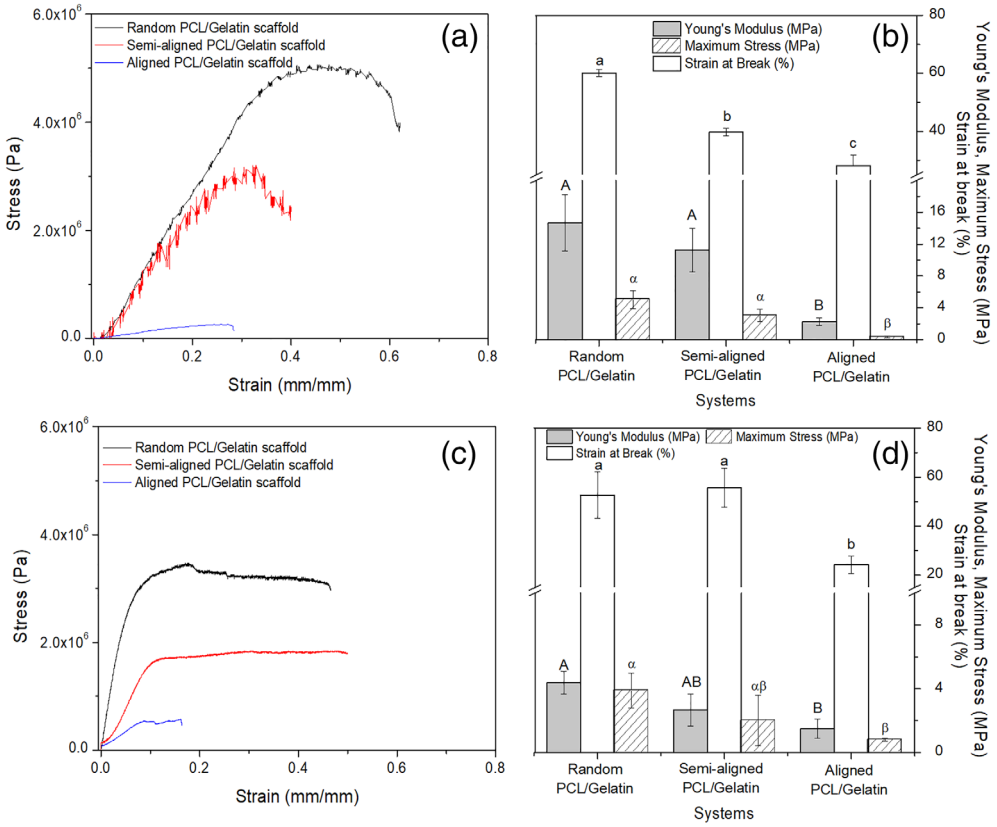

FIGURE 3 Strain–stress curves and parameters (Young's modulus, strain at break and maximum stress) obtained from the mechanical testing carried out under dry conditions for the polycaprolactone (PCL)/gelatin scaffolds produced with different alignments (random, semi-aligned and aligned) (a and b) before and after (c and d) a cyclic loading of 500 cycles at constant strain (10%) and frequency (1 Hz)

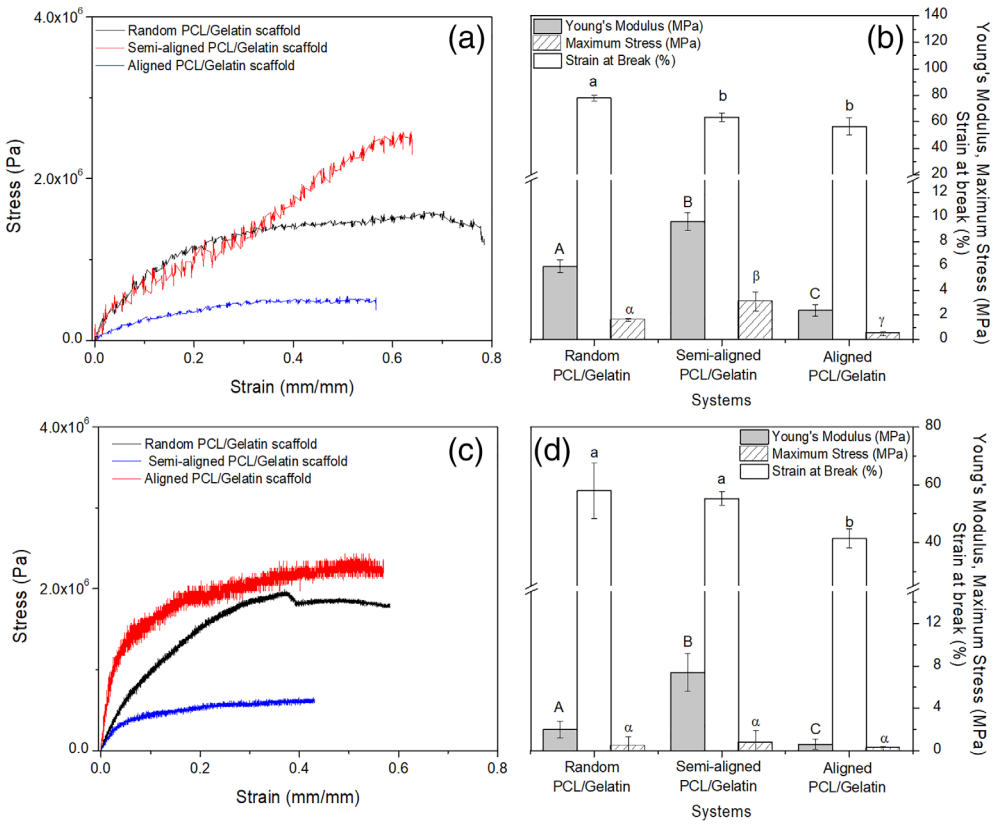

FIGURE 4 Strain–stress curves and parameters (Young's modulus, strain at break and maximum stress) obtained from the mechanical testing carried out under wet conditions for the polycaprolactone (PCL)/gelatin scaffolds produced with different alignments (random, semi-aligned and aligned) (a and b) before and after (c and d) a cyclic loading of 500 cycles at constant strain (10%) and frequency (1 Hz)

First, the evolution of the stress was followed all over the cycle under dry conditions (Figure 2(a)). According to the results shown in Table 2, the decrease in the stress for the three systems was below 5%: Random 4.9% (from 3.08 to 2.92 MPa), semi-aligned 2.3% (from 1.77 to 1.73 MPa), and aligned 3.9% (from 1.30 to 1.25 MPa). On the other hand, the cyclic loading test was also performed in wet conditions to evaluate the evolution of the stress with cycles (Figure 2(b)). Interestingly, the evolution of the stress showed a different trend

TABLE 3 Comparison of the Young's modulus, strain at break and maximum stress of the PCL/gelatin scaffolds produced with different alignments (random, semi-aligned and aligned)) before and after a cyclic loading of 500 cycles carried out under dry or wet conditions (strain of 10% and frequency of 1 Hz)

		Young's modulus (MPa)		Strain at break (%)		Maximum stress (MPa)	
SYSTEMS		Before	After	Before	After	Before	After
Random PCL/gelatin scaffold	Dry	14.9 ± 5.2^{a}	4.4 ± 0.4^{b}	66.3 ± 5.3^{A}	52.7 ± 9.6^{AE}	$4.4 \pm 0.4^{\alpha}$	$3.9 \pm 1.1^{\alpha\gamma}$
	Wet	5.1 ± 1.4^{b}	2.0 ± 0.8^{c}	77.9 ± 3.7^{B}	58.0 ± 8.6^{AE}	$1.4 \pm 0.7^{\beta}$	$0.4 \pm 0.9^{\beta\delta}$
Semi-aligned PCL/gelatin scaffold	Dry	11.3 ± 2.8^{a}	2.7 ± 1.0^{c}	39.7 ± 1.3^{C}	55.7 ± 7.85^{AE}	$3.0 \pm 0.8^{\gamma}$	$1.9 \pm 1.4^{\beta\delta}$
	Wet	9.6 ± 1.6^{a}	7.4 ± 1.8^{d}	63.5 ± 2.4^{A}	55.3 ± 2.47^{E}	$3.2 \pm 0.9^{\alpha\gamma}$	$0.7 \pm 1.2^{\beta\delta}$
Aligned PCL/gelatin scaffold	Dry	2.2 ± 0.6^{c}	1.7 ± 0.9^{c}	28.2 ± 3.6^{D}	24.3 ± 1.53^{D}	$0.4 \pm 0.2^{\delta}$	$0.8 \pm 0.1^{\beta}$
	Wet	2.4 ± 0.5^{c}	0.6 ± 0.5^{e}	56.5 ± 1.8^{E}	36.9 ± 3.29^{C}	$0.5 \pm 0.2^{\beta\delta}$	$0.2 \pm 0.2^{\delta}$

Note: Values with different letters are significantly different ($p < .05$).
Abbreviation: PCL, polycaprolactone.

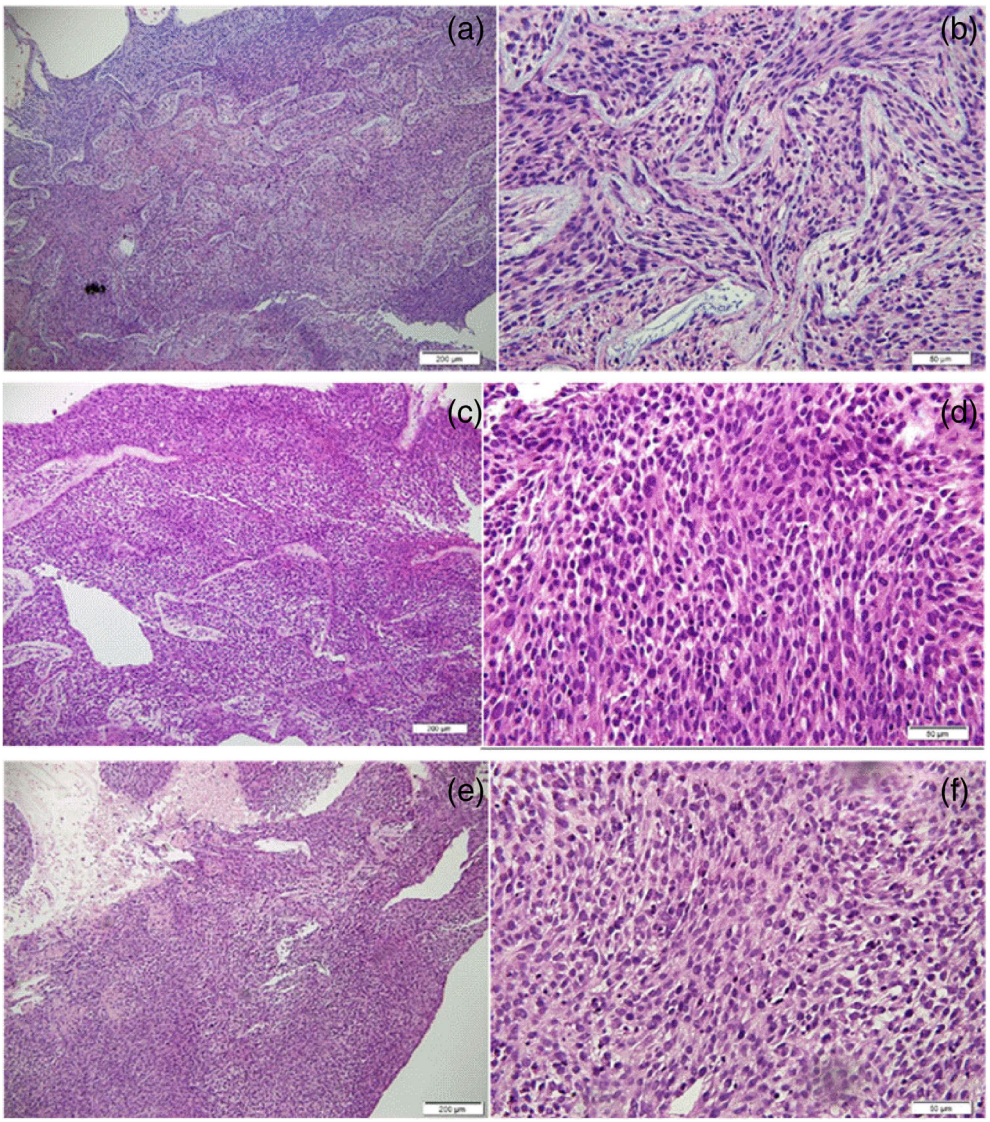

FIGURE 5 Haematoxylin–eosin (H&E) photomicrographs of the polycaprolactone (PCL)/gelatin scaffolds seeded with cells: (a, c and e) ×10 magnification and (b, d and f) ×40 magnification

compared to the cyclic loading performed under dry conditions. In this case, the system which suffered the greatest variation in the stress was the aligned one, with the random system showing the lowest variation. However, the observed decrease cannot be considered significant, since the maximum decrease obtained was below 2.5% (0.4, 1.6, and 2.2% for the random, semi-aligned, and aligned systems, respectively). These results may indicate that the cyclic loading was performed in the elastic region.

In addition to the cyclic loading, the different results obtained for the uniaxial tensile tests in dry conditions are plotted in Figure 3. Figure 3(a),(c) show the strain–stress curves of the PCL/gelatin scaffolds with different alignments. The profiles shown were similar, with an initial region with a high constant stress–strain slope (which corresponds to the elastic region), followed by a plastic region with a continuous decrease in the stress–strain slope toward a constant value. After reaching the maximum stress and maximum strain, the sample broke with a sudden decrease in stress. Furthermore, the different parameters obtained from the mechanical tests before and after the cyclic loading are shown in Figure 3(b),(c). Both experiments showed the same trend, that is a general decrease of the values with the alignment of the fibers, especially for the strain at break. In addition, two different trends can be observed when comparing the results obtained before and after the cyclic loading. Both Young's modulus and maximum stress showed a slight decrease after the cyclic loading, whereas strain at break showed no significant changes.

On the other hand, a comparison between the uniaxial tensile strength experiments carried out under wet conditions before and after the cyclic loading was also analyzed and the obtained results were plotted in Figure 4. A similar tendency can be seen in the evolution of the parameters since Young's modulus and maximum stress presented maximum values for the semi-aligned system, whereas strain at break decreased with the increase of the alignment.

Comparing the values under dry and wet conditions, different effects can be observed depending on the parameter studied (Table 3). First, there was an increase in the strain at break of the samples when performing the mechanical tests in wet conditions. This increase was more pronounced with the alignment of the fibers, with an average ratio of 1.75 for the aligned system compared to the values obtained for the semi-aligned and random systems, with an increase of 1.45 and 1.15, respectively. However, all the systems showed a decrease in maximum stress under wet conditions. In this case, the effect was more pronounced when the fibers were randomly distributed (average ratio decrease of 6.5, much higher than the values around 1.5–2.0 for the semi-aligned and aligned systems). Finally, Young's modulus showed a decrease under wet conditions for all the samples with an average ratio decrease between 1.0 and 3.0, except for the semi-aligned system after the cyclic loading, which increased its Young's modulus.

3.3 | Biological evaluation of nanofibrous scaffolds

A bioreactor that provides mechanical loading stimuli was used in this study, in order to achieve a greater expansion of cells in culture, thus improving cell population and differentiation, therefore increasing tissue production *in vitro*.

In general, viable cells with a good cell density were observed by H&E staining (Figure 5(a),(b)). Moreover, cell colonies had a lower alignment, corresponding to the properties of the scaffolds. In the semi-aligned scaffolds, most cells were viable and homogeneously

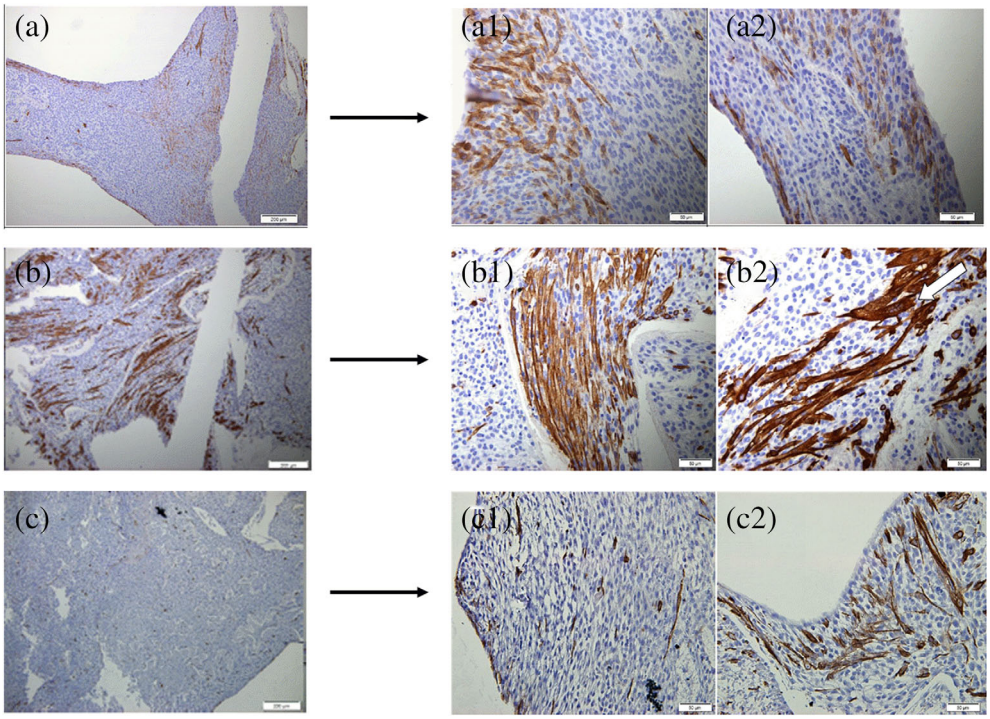

FIGURE 6 Immunohistochemical (IHC) staining images of the polycaprolactone (PCL)/gelatin scaffolds processed with different alignments: random (a, a1-a2), semi-aligned (b, b1-b2) and aligned (c, c1-c2) at ×10 and ×40, respectively

distributed with good cell density (Figure 5(c),(d)). These systems presented minimal foci of necrosis. On the other hand, the images corresponding to the aligned scaffolds (Figure 5(e),(f)) showed viable cells with homogeneous distribution, yet cells with rounded morphology, retracted cytoplasm and pyknotic nuclei could be seen in different areas as more foci of necrosis (60 ± 4% of viable cells) compared to the semi-aligned and random scaffolds (90 ± 5% and 70 ± 7% of viable cells, respectively).

In addition to H&E staining, immunohistochemical staining (IHC) was also carried out to study the degree of cell differentiation with smooth muscle actin (SMA) staining. Random scaffolds (Figures 6(a), (a1), and (a2)) had areas where the SMA was expressed, although very scarcely and mostly by the edges of the scaffolds. Cells seeded in the semi-aligned and aligned scaffolds expressed SMA more abundantly (Figures 6(a), (b1), (b2), (c1), (c2)).

4 | DISCUSSION

4.1 | Influence of the addition of collagen and gelatin

The results evidenced an increase in *nitrogen (N)* when the concentration of the used protein was higher (either collagen or gelatin). The increase in *N* content was more remarkable for the scaffolds with gelatin. In addition, the presence of protein was also identified by the FTIR profiles, being similar to the one obtained in a study carried out by Aguirre-Chagala et al. (2017) with combinations of PCL and collagen.[24] This profile is characterized by the presence of additional peaks which corresponded to the typical bands of proteins. Interestingly, the intensity of these signals increased when the protein used (either gelatin or collagen) was present at a higher concentration. Considering the surface wettability measurements, the addition of gelatin produced a remarkable decrease of the contact angle, which resulted in more hydrophilic scaffolds obtained when the amount of gelatin was higher. This hydrophilic character is more suitable for cell adhesion, as reported by Quigley et al. (2013),[39] with ideal contact angle values ranging from 40–70°. On the other hand, the addition of collagen did not produce a decrease in the contact angle of scaffolds, as previously shown by Dulnik et al. (2016).[40] This effect may be due to two different aspects: on the one hand, collagen is not so homogeneously located on the surface, which explains the low variation of the contact angle. On the other hand, gelatin has a higher content in glycine, valine and alanine amino acids, which allows the reorganization of the hydrophobic groups of proteins giving rise to a more hydrophilic structure, thus lowering the contact angle.[41]

Considering the microstructure, the addition of a protein caused a broader distribution and greater heterogeneity in the size of the fibers. This widening effect was also observed by other authors such as Gautam et al. (2013), in which combinations of PCL and gelatin led to electrospun fibers with a heterogeneous fiber size distribution, and an average value between 0.2 and 0.4 μm.[42] Among the different systems evaluated, the scaffolds produced with 4% of gelatin can be highlighted because its fiber size range was found to present a better cell behavior with electrospun scaffolds according to the studies of Chen et al. (2013).[43]

The evaluation of the mechanical properties also revealed that the system with a 4% of gelatin could be suitable for cell growth since, although a decrease in both Young's modulus and maximum stress is observed, an increase in the strain at break is also observed. This increase would lead to a better response of the scaffold in the bioreactor, because it is highly recommended the use of scaffolds that present good deformability to be able to withstand the mechanical stimulation of the bioreactor without breaking.

4.2 | Influence of the alignment of electrospun scaffolds

Regarding the characterization of the hybrid PCL/protein-based systems, it can be concluded that the PCL/gelatin (4%) system is particularly interesting due to the properties described above: It presented a homogeneous and suitable fiber size distribution and an ideal hydrophilicity for optimal cell interaction. In addition, the Young's modulus obtained for this system is similar to that obtained by Du et al. (2018) in their study with skeletal muscle cells.[44] For these reasons, it was selected to analyze the influence of the fiber alignment.

The characterization of the systems with different alignments revealed a Gaussian distribution ranged between 200 and 400 nm. This range is similar as what obtained by other PCL/gelatin scaffolds,[29] but lower than the range found by Gomes et al. (2017) in their ternary systems for skin tissue engineering.[45] Comparing the contact angle values of the PCL/gelatin scaffolds with different alignments, a decrease was observed with the increasing alignment of the scaffolds. According to the ideal range found by Quigley et al.

TABLE 4 Comparative results (cell population, cell viability, cell area and occupation) obtained staining image of the PCL/gelatin scaffolds processed with different alignments: random, semi-aligned and aligned

SYSTEMS	Cell population	Cell viability (%)	Cell area (μm^2)	Occupation (%)
Random PCL/gelatin scaffold	1,217 $^{\alpha}$	71.7 ^{A}	23.96 ^{a}	22 ^{I}
Semi-aligned PCL/gelatin scaffold	1,220 $^{\alpha}$	86.7 ^{B}	27.86 ^{b}	23 ^{I}
Aligned PCL/gelatin scaffold	1,194 $^{\alpha}$	57.5 ^{C}	26.59 ^{ab}	21 ^{I}

Note: Values with different letters are significantly different ($p < 0.05$).
Abbreviation: PCL, polycaprolactone.

(2013),[39] a suitable wettability is obtained by the random and semi-aligned systems.

According to the mechanical properties measured for these systems, Young's moduli obtained are slightly lower than the values obtained by Reddy et al. (2014) for their PCL-based structures for cardiac tissue engineering, but with similar maximum stress value (around 1.5–2.5 MPa).[46] In fact, analyzing the evolution of the parameters after the cyclic loading, a general decrease of the properties was observed, especially for Young's modulus and strain at break. The differences found in the stress–strain curves for the random and semi-aligned systems (Figure 4) may be produced by a combination of two effects: The hydrophilic character of gelatin and the reorganization of the nanofibers. The initial partial orientation of the fibers of the semi-aligned system (produced by the rotational speed of the collector during the fabrication of the scaffolds) may induce a reorganization of the fibers, which leads to nodes of nanofibers connected and oriented in several directions. These nodes may act as stress accumulators and propagators, allowing the scaffold to withstand greater stress.[47] This effect is more significative for the semi-aligned system and in wet conditions due to the hydrophilic character of gelatin allowing it to swell. Combined with the original partial orientation, this induces obtaining greater nodes; hence, a greater stress can be withstood. These results suggest that nanofibrous scaffolds present higher deformability and lower rigidity in a wet environment, compared to their behavior in dry conditions. In conclusion, considering the obtained results, a certain alignment of the fibers induced an increase in the mechanical properties. In fact, the parameters (Young's modulus, maximum stress and strain at break) reached their maximum values for those scaffolds formed by nanofibers with an intermediate alignment (semi-aligned scaffolds). An excessive alignment would lead to an anisotropic material showing a tendency to break in specific sites, which should be taken into account in future biological studies.

4.3 | Biological evaluation of nanofibrous scaffolds

A bioreactor was used to provide mechanical stimuli on the scaffolds during cell growth since some studies carried out by Bach et al. demonstrated the beneficial effect of mechanical stimuli on the formation of differentiated functional muscle tissue.[48] The biological evaluation of the selected systems showed that fiber alignment did not influence cell growth of the scaffolds (Table 4). Cell viability and cell area improved when an intermediate alignment was used (semi-aligned systems). However, IHC staining revealed that random scaffolds presented few fusiform cells, characteristic of myotubules; this may be due to the low percentage of alignment, which does not favor cell fusion. On the other hand, more fusiform cells could be seen in the semi-aligned and aligned structures, as result of the formation of functional myotubules, induced by the alignment and the application of the bioreactor during cell growth, as also shown by Powell et al.[49] In case of aligned scaffolds, SMA was predominately expressed at the edges. Isolated cells with fusiform shape could be also observed.

5 | CONCLUSIONS

Hybrid nanofibrous protein-PCL scaffolds with different concentrations of gelatin and collagen were obtained by electrospinning, showing potential for applications in tissue engineering. EDAX measurements revealed that the systems produced with a higher concentration of protein presented a higher protein content in the final scaffolds. In general, a higher protein content was observed in the gelatin-based scaffolds compared to the collagen ones. In addition, the hydrophilicity of PCL scaffolds can be enhanced with the addition of gelatin to their initial formulation, due to the hydrophilic character of this protein.

Hybrid protein-PCL scaffolds presented lower fiber size and, consequently, lower porosity. Lower fiber sizes are more suitable to obtain a larger surface for cell adhesion. Consequently, there was a general reduction of the mechanical properties of PCL-based scaffolds, dominated by the presence of proteins (either gelatin or collagen) in the fibers, obtaining scaffolds with a Young's modulus or maximum stress up to four times lower than that of pure PCL scaffolds. In fact, the addition of gelatin produced more deformable scaffolds with lower stiffness.

The biological evaluation revealed the possibility to create *ex vivo* skeletal muscle tissue using a bioreactor. Fiber alignment did not influence cell proliferation *in vitro*. However, the alignment of the fibers played an important role in cell growth and viability. Cell viability and differentiation were promoted to a greater extent in the semi-aligned scaffolds as compared to the random and aligned scaffolds. PCL + Gelatin (4%) scaffolds seemed to be the most appealing mixture. The biological evaluation of these scaffolds revealed that they are suitable to harbor cells and, consequently, to develop tissues. Further research will involve testing the scaffolds in an animal mode to further examine biological functionality.

ACKNOWLEDGMENTS

This work is part of a research project sponsored by "Ministerio de Economía y Competitividad" (MINECO/FEDER, EU) from the Spanish Government (Ref. CTQ2015-71164-P). The authors gratefully acknowledge their financial support. The authors also acknowledge Universidad de Sevilla for the VPPI-US grant of Victor M. Perez-Puyana. Part of this work was carried out at the Department of Complex Tissue Regeneration (MERLN Institute for Technology-Inspired Regenerative Medicine, Maastricht University) and with financial support from the program *"Estancias breves en España y en el extranjero para beneficiarios de Becas predoctorales o PIF de la US y de Becas de la Fundación Cámara"* from the Universidad de Sevilla. This research project was made possible by the Dutch Province of Limburg (LINK program).

AUTHOR CONTRIBUTIONS

Conceptualization, V. Perez-Puyana and P. Wieringa; methodology, V. Perez-Puyana; software, V. Perez-Puyana and Y. Yuste; validation, P. Wieringa and A. Romero; formal analysis, P. Wieringa and A. Romero; investigation, V. Perez-Puyana and Y. Yuste; resources, L. Moroni and F. de la Portilla; biological supervision, F. de la Portilla; writing—original draft preparation, V. Perez-Puyana and Y. Yuste; visualization, P. Wieringa and A. Romero; writing—review and editing,

P. Wieringa, F. de la Portilla, A. Romero, A. Guererro and L. Moroni; supervision, L. Moroni, P. Wieringa, and A. Guererro; funding acquisition, F. de la Portilla, A. Guererro and L. Moroni.

DATA AVAILABILITY STATEMENT

Data are available upon request.

REFERENCES

1. Qazi TH, Duda GN, Ort MJ, Perka C, Geissler S, Winkler T. Cell therapy to improve regeneration of skeletal muscle injuries. *J Cachexia Sarcopenia Muscle*. 2019;*10*:501-516.
2. Bailey P, Holowacz T, Lassar AB. The origin of skeletal muscle stem cells in the embryo and the adult. *Curr Opin Cell Biol*. 2001;*13*:679-689. https://linkinghub.elsevier.com/retrieve/pii/S0955067400002714.
3. Saihara R, Komuro H, Urita Y, Hagiwara K, Kaneko M. Myoblast transplantation to defecation muscles in a rat model: a possible treatment strategy for fecal incontinence after the repair of imperforate anus. *Pediatr Surg Int*. 2009;*25*:981. https://doi.org/10.1007/s00383-009-2454-3.
4. Aghaee-Afshar M, Rezazadehkermani M, Asadi A, Malekpour-Afshar R, Shahesmaeili A, Nematollahi-mahani SN. Potential of human umbilical cord matrix and rabbit bone marrow-derived mesenchymal stem cells in repair of surgically incised rabbit external anal sphincter. *Dis Colon Rectum*. 2009;*52*:1753-1761.
5. Bisson A, Freret M, Drouot L, et al. Restoration of anal sphincter function after myoblast cell therapy in incontinent rats. *Cell Transplant*. 2015;*24*:277-286.
6. Frudinger A, Kolle D, Schwaiger W, Pfeifer J, Paede J, Halligan S. Muscle-derived cell injection to treat anal incontinence due to obstetric trauma: pilot study with 1 year follow-up. *Gut*. 2010;*59*:55-61.
7. Zadpoor AA. The evolution of biomaterials research. *Mater Today*. 2013;*16*:408-409. https://doi.org/10.1016/j.mattod.2013.10.015.
8. Chia HN, Wu BM. Recent advances in 3D printing of biomaterials. *J Biol Eng*. 2015;*9*:1-14.
9. O'Brien FJ, Harley BA, Yannas IV, Gibson L. Influence of freezing rate on pore structure in freeze-dried collagen-GAG scaffolds. *Biomaterials*. 2004;*25*:1077-1086.
10. Zhang S. Fabrication of novel biomaterials through molecular self-assembly. *Nat Biotechnol*. 2003;*21*:1171-1178.
11. De Vrieze S, Van Camp T, Nelvig A, Hagström B, Westbroek P, De Clerck K. The effect of temperature and humidity on electrospinning. *J Mater Sci*. 2009;*44*:1357-1362.
12. De la Portilla F, Pereira S, Molero M, et al. Microstructural, mechanical, and histological evaluation of modified alginate-based scaffolds. *J Biomed Mater Res-Part A*. 2016;*104*:3107-3114.
13. Jin G, He R, Sha B, et al. Electrospun three-dimensional aligned nanofibrous scaffolds for tissue engineering. *Mater Sci Eng C*. 2018;*92*:995-1005.
14. Zhang X, Tang K, Zheng X. Electrospinning and crosslinking of COL/-PVA nanofiber-microsphere containing salicylic acid for drug delivery. *J Bionic Eng*. 2016;*13*:143-149. https://doi.org/10.1016/S1672-6529(14)60168-2.
15. Alhosseini SN, Moztarzadeh F, Mozafari M, et al. Synthesis and characterization of electrospun polyvinyl alcohol nanofibrous scaffolds modified by blending with chitosan for neural tissue engineering. *Int J Nanomedicine*. 2012;*7*:25-34.
16. Dowling DP, Miller IS, Ardhaoui M, Gallagher WM. Effect of surface wettability and topography on the adhesion of osteosarcoma cells on plasma-modified polystyrene. *J Biomater Appl*. 2011;*26*:327-347.
17. Agarwal R, Alam MS, Gupta B. Polyvinyl alcohol-polyethylene oxide-carboxymethyl cellulose membranes for drug delivery. *J Appl Polym Sci*. 2013;*129*:3728-3736.
18. Pimentel MR, Falcone S, Cadot B, Gomes ER. In vitro differentiation of mature myofibers for live imaging. *J Vis Exp*. 2017;*119*:55141. https://doi.org/10.3791/55141.
19. Barrère F, Mahmood TA, de Groot K, van Blitterswijk CA. Advanced biomaterials for skeletal tissue regeneration: instructive and smart functions. *Mater Sci Eng R Rep*. 2008;*59*:38-71. Available from. http://www.sciencedirect.com/science/article/pii/S0927796X07001234.
20. Lee CH, Singla A, Lee Y. Biomedical applications of collagen. *Int J Pharm*. 2001;*221*:1-22. Available from:. http://www.sciencedirect.com/science/article/pii/S0378517301006913.
21. Plunkett N, O'Brien FJ. Bioreactors in tissue engineering. *Technol Health Care*. 2011;*19*:55-69.
22. Kasper C, Van Griensven M, Pörtner R. *Bioreactor Systems for Tissue Engineering*. Berlin Heidelberg: Springer; 2009.
23. Akhyari P, Fedak P, Weisel R, et al. Mechanical stretch regimen enhances the formation of bioengineered autologous cardiac muscle grafts. *Circulation*. 2002;*106*:I137-I142.
24. Aguirre-Chagala YE, Altuzar V, León-Sarabia E, Tinoco-Magaña JC, Yañez-Limón JM, Mendoza-Barrera C. Physicochemical properties of polycaprolactone/collagen/elastin nanofibers fabricated by electrospinning. *Mater Sci Eng C*. 2017;*76*:897-907. Available from. https://doi.org/10.1016/j.msec.2017.03.118.
25. Gümüşderelioğlu M, Dalkıranoğlu S, Aydın RST, Çakmak S. A novel dermal substitute based on biofunctionalized electrospun PCL nanofibrous matrix. *J Biomed Mater Res Part A*. 2011;*98A*:461-472.
26. Woodruff MA, Hutmacher DW. The return of a forgotten polymer—polycaprolactone in the 21st century. *Prog Polym Sci*. 2010;*35*:1217-1256. Available from. https://www.sciencedirect.com/science/article/pii/S0079670010000419.
27. Hendrikson WJ, Rouwkema J, Van Blitterswijk CA, Moroni L. Influence of PCL molecular weight on mesenchymal stromal cell differentiation. *RSC Adv*. 2015;*5*:54510-54516. Available from. https://doi.org/10.1039/C5RA08048G.
28. Manikandan S, Divyabharathi M, Tomas K, Pavel P, David L. Production of poly (ϵ-caprolactone) antimicrobial nanofibers by needleless alternating current electrospinning. *Mater Today Proc*. 2019;*17*:1100-1104. Available from. https://doi.org/10.1016/j.matpr.2019.06.526.
29. Ren K, Wang Y, Sun T, Yue W, Zhang H. Electrospun PCL/gelatin composite nanofiber structures for effective guided bone regeneration membranes. *Mater Sci Eng C*. 2017;*78*:324-332. Available from. https://doi.org/10.1016/j.msec.2017.04.084.
30. Sant S, Hwang CM, Lee S-H, Khademhosseini A. Hybrid PGS-PCL microfibrous scaffolds with improved mechanical and biological properties. *J Tissue Eng Regen Med*. 2011;*5*:283-291.
31. Annabi N, Fathi A, Mithieux SM, Weiss AS, Dehghani F. Fabrication of porous PCL/elastin composite scaffolds for tissue engineering applications. *J Supercrit Fluids*. 2011;*59*:157-167. Available from. https://doi.org/10.1016/j.supflu.2011.06.010.
32. Allam E, Bottino MC, Al-Shibani N, Jack Windsor L. Collagen scaffolds: tissue engineering and repair type I collagen. *Biol Funct Synth Med Appl*. 2012;*1*:145-157.
33. Hartman O, Zhang C, Adams EL, et al. Biofunctionalization of electrospun PCL-based scaffolds with perlecan domain IV peptide to create a 3-D pharmacokinetic cancer model. *Biomaterials*. 2010;*31*:5700-5718.
34. Chong C, Wang Y, Fathi A, Parungao R, Maitz PK, Li Z. Skin wound repair: results of a pre-clinical study to evaluate electropsun collagen-elastin-PCL scaffolds as dermal substitutes. *Burns*. 2019;*45*:1639-1648.
35. Pandey S, Rathore K, Johnson J, Cekanova M. Aligned nanofiber material supports cell growth and increases osteogenesis in canine adipose-derived mesenchymal stem cells in vitro. *J Biomed Mater Res A*. 2018;*106*:1780-1788.

36. Meng ZX, Wang YS, Ma C, Zheng W, Li L, Zheng YF. Electrospinning of PLGA/gelatin randomly-oriented and aligned nanofibers as potential scaffold in tissue engineering. *Mater Sci Eng C*. 2010;*30*:1204-1210.
37. Duque Sánchez LM, Rodriguez L, López M. Electrospinning: the Nanofibers age. *Rev Iberoam Polímeros Vol Iber Polímeros*. 2014;*14*: 10-27.
38. Perez-Puyana V, Jiménez-Rosado M, Romero A, Guerrero A. Development of PVA/gelatin nanofibrous scaffolds for tissue engineering via electrospinning. *Mater Res Express*. 2018;*5*:035401.
39. Quigley AF, Wagner K, Kita M, et al. In vitro growth and differentiation of primary myoblasts on thiophene based conducting polymers. *Biomater Sci*. 2013;*1*:983-995.
40. Dulnik J, Denis P, Sajkiewicz P, Kołbuk D, Choińska E. Biodegradation of bicomponent PCL/gelatin and PCL/collagen nanofibers electrospun from alternative solvent system. *Polym Degrad Stab*. 2016;*130*:10-21.
41. Southall NT, Dill KA, Haymet ADJ. A view of the hydrophobic effect. *J Phys Chem B*. 2002;*106*:521-533.
42. Gautam S, Dinda AK, Mishra NC. Fabrication and characterization of PCL/gelatin composite nanofibrous scaffold for tissue engineering applications by electrospinning method. *Mater Sci Eng C*. 2013;*33*: 1228-1235. Available from. https://doi.org/10.1016/j.msec.2012.12.015.
43. Chen MC, Sun YC, Chen YH. Electrically conductive nanofibers with highly oriented structures and their potential application in skeletal muscle tissue engineering. *Acta Biomater*. 2013;*9*:5562-5572. Available from. https://doi.org/10.1016/j.actbio.2012.10.024.
44. Du Y, Ge J, Li Y, Ma PX, Lei B. Biomimetic elastomeric, conductive and biodegradable polycitrate-based nanocomposites for guiding myogenic differentiation and skeletal muscle regeneration. *Biomaterials*. 2018;*157*:40-50. Available from. https://doi.org/10.1016/j.biomaterials.2017.12.005.
45. Gomes S, Rodrigues G, Martins G, Henriques C, Silva JC. Evaluation of nanofibrous scaffolds obtained from blends of chitosan, gelatin and polycaprolactone for skin tissue engineering. *Int J Biol Macromol*. 2017;*102*:1174-1185. Available from. https://doi.org/10.1016/j.ijbiomac.2017.05.004.
46. Srinivasa Reddy C, Reddy Venugopal J, Ramakrishna S, Zussman E. Polycaprolactone/oligomer compound scaffolds for cardiac tissue engineering. *J Biomed Mater Res Part A*. 2014;*102*:3713-3725.
47. Wisnom MR, Green D. Tensile failure due to interaction between fibre breaks. *Composites*. 1995;*26*:499-508. Available from:. http://www.sciencedirect.com/science/article/pii/001043619596807I.
48. Bach AD, Stem-Straeter J, Beier JP, Bannasch H, Stark GB. Engineering of muscle tissue. *Clin Plast Surg*. 2003;*30*:589-599.
49. Powell CA, Smiley BL, Mills J, Vandenburgh HH. Mechanical stimulation improves tissue-engineered human skeletal muscle. *Am J Physiol cell Physiol*. 2002;*283*:C1557-C1565.

SUPPORTING INFORMATION

Additional supporting information may be found online in the Supporting Information section at the end of this article.

How to cite this article: Perez-Puyana V, Wieringa P, Yuste Y, et al. Fabrication of hybrid scaffolds obtained from combinations of PCL with gelatin or collagen via electrospinning for skeletal muscle tissue engineering. *J Biomed Mater Res*. 2021;109:1600–1612. https://doi.org/10.1002/jbm.a.37156